AFRL-RV-PS-
TR-2018-0022

SPACE PLATFORMS & OPERATIONS TECHNOLOGIES

Kathleen Howell and Theodore Wahl

Purdue University
401 South Grant Street
West Lafayette, IN 47907-2024

02 April 2018

Final Report

AIR FORCE RESEARCH LABORATORY
Space Vehicles Directorate
3550 Aberdeen Ave SE
AIR FORCE MATERIEL COMMAND
KIRTLAND AIR FORCE BASE, NM 87117-5776

NOTICE AND SIGNATURE PAGE

Using Government drawings, specifications, or other data included in this document for any purpose other than Government procurement does not in any way obligate the U.S. Government. The fact that the Government formulated or supplied the drawings, specifications, or other data does not license the holder or any other person or corporation; or convey any rights or permission to manufacture, use, or sell any patented invention that may relate to them.

This report is the result of contracted fundamental research which is exempt from public affairs security and policy review in accordance with AFI 61-201, paragraph 2.3.5.1. This report is available to the general public, including foreign nationals. Copies may be obtained from the Defense Technical Information Center (DTIC) (http://www.dtic.mil).

AFRL-RV-PS-TR-2018-0022 HAS BEEN REVIEWED AND IS APPROVED FOR PUBLICATION IN ACCORDANCE WITH ASSIGNED DISTRIBUTION STATEMENT.

//SIGNED//
RICHARD ERWIN
Program Manager

//SIGNED//
PAUL HAUSGEN
Tech Advisor, Spacecraft Component Technology Branch

//SIGNED//
JOHN BEAUCHEMIN
Chief Engineer, Spacecraft Technology Division
Space Vehicles Directorate

This report is published in the interest of scientific and technical information exchange, and its publication does not constitute the Government's approval or disapproval of its ideas or findings.

Approved for public release; distribution is unlimited.

REPORT DOCUMENTATION PAGE

Form Approved
OMB No. 0704-0188

1. REPORT DATE *(DD-MM-YY)*	**2. REPORT TYPE**	**3. DATES COVERED** *(From - To)*
02-04-2018	Final Report	02 Oct 2014 – 02 Apr 2018

4. TITLE AND SUBTITLE
Space Platforms & Operations Technologies

5a. CONTRACT NUMBER

5b. GRANT NUMBER
FA9453-15-1-0306

5c. PROGRAM ELEMENT NUMBER
62601F

6. AUTHOR(S)
Kathleen Howell and Theodore Wahl

5d. PROJECT NUMBER
8809

5e. TASK NUMBER
PPM00019267

5f. WORK UNIT NUMBER
EF122155

7. PERFORMING ORGANIZATION NAME(S) AND ADDRESS(ES)

Purdue University
401 South Grant Street
West Lafayette, IN 47907-2024

8. PERFORMING ORGANIZATION REPORT NUMBER

9. SPONSORING / MONITORING AGENCY NAME(S) AND ADDRESS(ES)

Air Force Research Laboratory
Space Vehicles Directorate
3550 Aberdeen Ave., SE
Kirtland AFB, NM 87117-5776

10. SPONSOR/MONITOR'S ACRONYM(S)
AFRL/RVSV

11. SPONSOR/MONITOR'S REPORT NUMBER(S)
AFRL-RV-PS-TR-2018-0022

12. DISTRIBUTION / AVAILABILITY STATEMENT
Approved for public release; distribution is unlimited.

13. SUPPLEMENTARY NOTES
FOA-RVKV-2013-0001, Space Platforms & Operations Technologies

14. ABSTRACT
A guidance strategy for autonomous spacecraft formation reconfiguration maneuvers solves the linked assignment and delivery problems. First, the member spacecraft in the formation are each assigned to their new positions in the desired formation geometry. The guidance algorithm then employs an auction process, with estimates for the maneuvers and times-of-flight, that minimize a specific "expense" function for the formation. To guide the spacecraft to their assigned positions, the first of two guidance schemes is based on artificial potential functions (APF). Using relative distances between the spacecraft, targets, and any obstacles, the APF approach yields maneuvers based on gradients of the potential field. The second delivery scheme leverages model predictive control. The guidance algorithm uses an analytical linearized approximation of the relative orbital dynamics, the Yamanaka-Ankersen state transition matrix, in the auction process and in both delivery methods. The proposed guidance strategy is successful, in simulations, in autonomously assigning the members of the formation to new positions and in delivering the spacecraft to these new positions safely using both delivery methods.

15. SUBJECT TERMS
Adaptive Artificial Potential Function; AAPF; Artificial Potential Functions; APF; Multiple-Target APF; Single Target APF; Spacecraft Formation Flying; Model Predictive Control; MPC and Formation Reorientation

16. SECURITY CLASSIFICATION OF:			**17. LIMITATION OF ABSTRACT**	**18. NUMBER OF PAGES**	**19a. NAME OF RESPONSIBLE PERSON**
					Richard S. Erwin
a. REPORT	**b. ABSTRACT**	**c. THIS PAGE**	Unlimited	42	**19b. TELEPHONE NUMBER** *(include area code)*
Unclassified	Unclassified	Unclassified			

(This page intentionally left blank)

TABLE OF CONTENTS

Section **Page**

LIST OF FIGURES

Figure **Page**

LIST OF TABLES

Table **Page**

ACKNOWLEDGMENTS AND DISCLAIMER

This material is based on research sponsored by Air Force Research Laboratory (AFRL) under agreement number FA9453-15-1-0306. The U.S. Government is authorized to reproduce and distribute reprints for Governmental purposes notwithstanding any copyright notation thereon.

The views and conclusions contained herein are those of the authors and should not be interpreted as necessarily representing the official policies or endorsements, either expressed or implied, of Air Force Research Laboratory (AFRL) or the U.S. Government.

1 SUMMARY

The objective of this investigation is to create an autonomous, decentralized guidance algorithm for a formation reconfiguration maneuver of an arbitrary number of satellites. The algorithm must handle the twin problems of assignment and delivery. The current algorithm uses an auction process to assign the spacecraft to new positions in the formation. This auction bases its bidding around the estimated ΔV and the estimated time of flight for each transfer. The algorithm then uses either artificial potential functions (APF) or model predictive control (MPC) to design the maneuvers that deliver the spacecraft safely to its new position. The APF and MPC guidance strategies both utilize the Yamanaka-Ankersen approximation of orbital relative motion. In simulations under Keplerian and perturbed dynamics, the guidance algorithm is successful in guiding formations through reconfiguration maneuvers; it requires from the operator only the initial spacecraft state information and desired new formation geometry to perform the maneuver. Both APF and MPC have parameters that can be tuned to better suit different scenarios. Current work is focused on determining the optimal ranges of these parameters, along with which scenarios are suited to APF or MPC delivery methods.

2 INTRODUCTION

The options afforded by satellites or spacecraft operating in formation is an important development that may allow new civilian and military operational capabilities; autonomous, decentralized control and guidance for these formations is essential to the success of such operations. Current formation flying missions include: Prototype Research Instruments and Space Mission Technology Advancement PRISMA, Cluster, and the Magnetospheric Multiscale (MMS) Mission.[1, 2, 3] In recent years, other mission concepts have also been explored including the developments for Terrestrial Planet Finder (TPF) from NASA and Darwin by ESA.[4, 5] Closer to Earth, TechSat-21 was a planned Air Force satellite mission to demonstrate formation flying technology.[6] Spacecraft formations have, in fact, long been investigated for mission scenarios that cannot be accomplished by a single vehicle; cooperating formations are potentially more robust and adaptable than single monolithic spacecraft. However, multiple spacecraft operating in close proximity also introduce additional complexities. To quickly and efficiently operate in such environments, guidance and control algorithms that operate autonomously are also a key capability. Thus, a decentralized autonomous guidance algorithm for formation maneuvers is examined.

For the development of this formation guidance system, two problems have traditionally been identified that any such algorithm must solve. The first is defined as the "assignment problem", i.e., assigning the spacecraft in the formation to their new positions. A satisfying solution to the assignment problem fills all the positions in the formation such that overall propellant consumption, time of flight, or some combination of both is minimized. The next step is a solution to the "delivery problem", that is, the task of delivering each spacecraft to their assigned positions by balancing the maneuver cost (ΔV) and travel time while avoiding collisions between the spacecraft and any other orbital objects. For this investigation, the goal is the creation of a straightforward guidance strategy for autonomous delivery of the reconfiguration maneuvers for formations of spacecraft. The manifestation of this strategy is a guidance algorithm that performs simulated reconfiguration maneuvers. This analysis addresses this goal through three main objectives: Creation of a scheme to assign spacecraft to positions in the formation, creation of methodologies to deliver the spacecraft to their new positions, and evaluation of the guidance algorithm in varied scenarios.

In the overarching strategy, the assignment problem is addressed through an auction process; auction algorithms are a well-accepted approach for solving the classical assignment problem, that is, matching n spacecraft and n target positions.[7, 8] A cost is associated with every spacecraft-target combination, and each target carries a price. The cost of each pairing between spacecraft and target is determined by a combination of the estimated ΔV and the estimated time of flight for that pairing. The spacecraft "satisfaction" with its assignment is based on the trade-off between cost and price. Initially unassigned, a simple algorithm is employed to allow a spacecraft to bid on the targets that result in the most spacecraft satisfaction. Then, each target selects the spacecraft with the largest bid; the target price increases based on the winning bid, and the process repeats for all spacecraft that remain unassigned. As the auction continues and the targets receive new bids, the assignments change, and the prices rise–changing the calculus of desirability. The algorithm terminates when all spacecraft are assigned to targets. In an update to the authors' previous work,[9] the improved auction algorithm avoids initialization bias in the assignments and accommodates a broader spectrum of formations–uneven numbers of spacecraft and targets or restrictions on spacecraft-target pairing, for example.

The second task in any reconfiguration problem is the "delivery problem," i.e., delivering each spacecraft to its assigned position. Any guidance strategy that supports a formation of vehicles operating autonomously must be sufficiently straightforward in terms of the on-board computational requirements while still offering accurate and propellant-efficient

relative trajectory computations and delivery. Simultaneously, the complexity involving multiple vehicles in the likely operational environment implies continually evolving relative motions yet includes constraints on both the path and the time of flight. Two strategies to achieve delivery of the vehicles are examined. The first is based on Artificial Potential Function (APF) guidance and is similar to a previously introduced technique.[9] Alternatively, a second approach involves Model Predictive Control (MPC). Of course, both guidance schemes possess advantages and disadvantages. Wahl develops the complete details,[10] but the results of the complete effort are presented in this work. A review of the dynamics of relative motion in Earth orbit first offers an introduction to the problem. The relative motion equations are briefly summarized in terms of suitable approximations–including the Yamanaka-Ankersen relative motion model–used in the auction and delivery processes, along with the impact of orbital perturbations. The mathematical foundations and the performances of the two delivery methods, MPC and APF, are introduced and compared. The auction algorithm applied to the assignment problem is detailed; the most useful improvements are emphasized. Finally, the status and ongoing efforts are noted.

3 METHODS, ASSUMPTIONS, PROCEEDURES

3.1 Relative Motion

For a formation of spacecraft, accurately modeling the relative motion is a necessity for any guidance strategy. To represent the relative motion of spacecraft orbiting the Earth, the Hill or Local-Vertical Local-Horizontal (LVLH) frame is typically employed. The Hill frame is a reference frame with an origin at a spacecraft as it orbits the Earth. For a formation, let one spacecraft be designated the "chief" while the others are denoted as "deputies." It is not required that the chief be a physical vehicle, rather, it may exist simply as a reference orbit for the formation. The orbital motion of the chief serves as the basis for the definition of the Hill frame with the chief located at the origin. The $\hat{x}$-direction is then aligned with the radius vector directed from the Earth center toward the chief, the $\hat{z}$-direction is aligned with the chief's orbital angular momentum vector, and $\hat{y}$ completes the triad such that $\hat{y} = \hat{z} \times \hat{x}$. If the chief moves in a circular orbit, the $\hat{y}$ direction is aligned with the in-track velocity direction. The elements of the Hill frame are illustrated in Figure 1. The chief orbit is plotted in red, with the vector from Earth center to the chief labeled as $\mathbf{r}_C$ and the true anomaly corresponding to the chief orbit is represented by θ_C. In the Hill frame, the positions of the deputy spacecraft with respect to the chief are denoted by $\boldsymbol{\rho} = x\hat{x} + y\hat{y} + z\hat{z}$.. Note that, variables in bold type represent vectors, italic type reflect scalars, and carets indicate unit vectors.

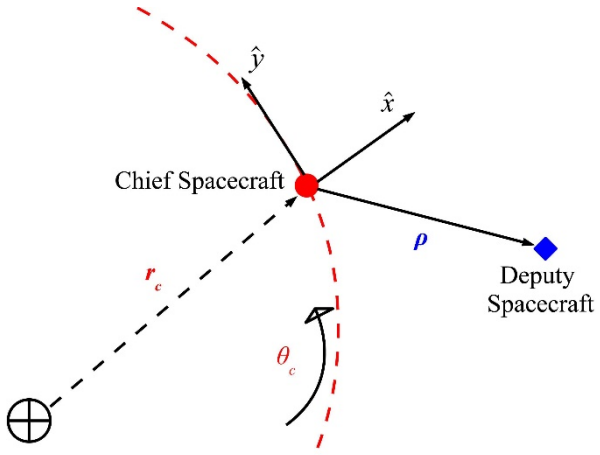

Figure 1. Schematic of the Hill Frame

3.1.1 Equations of Relative Motion

A representative dynamical model serves as the basis for any analysis, so the first task is to derive a set of variational equations of motion. Assuming the only force on the spacecraft is the force of gravity due to a spherically symmetric Earth, the equations of motion for a deputy spacecraft are derived and appear in the following form:

$$\ddot{x} = \frac{\mu}{{r_c}^2} + {\dot{\theta}_c}^2 x - 2\dot{\theta}_c\left(\frac{\dot{r}_c y}{r_c} - \dot{y}\right) - \frac{\mu}{{r_d}^3}(r_c + x) \tag{1}$$

$$\ddot{y} = {\dot{\theta}_c}^2 y - 2\dot{\theta}_c\left(\dot{x} - \frac{\dot{r}_c x}{r_c}\right) - \frac{\mu}{{r_d}^3} y \tag{2}$$

$$\ddot{z} = -\frac{\mu}{{r_d}^3} z \tag{3}$$

where μ is the gravitational parameter of Earth and r_d is the distance from Earth center to a deputy spacecraft–such that $r_d = \left[\left(r_c + x\right)^2 + y^2 + z^2\right]^{1/2}$. These equations incorporate the chief radial distance, r_C, and true anomaly, θ_C, that are determined from the conic equations:

$$\ddot{r}_c = \dot{\theta}_c^2 r_c - \frac{\mu}{r_c^2}, \qquad \ddot{\theta}_c = -\frac{2\dot{\theta}_c \dot{r}_c}{r_c} \tag{4}$$

Unless otherwise indicated, any simulations use the nonlinear equations of relative motion to represent the dynamics of spacecraft in the Hill frame. These equations of motion are valid for any chief moving on a Keplerian orbit and require no assumptions about the chief eccentricity.

To avoid relative drift, it is necessary that the vehicles within the formation remain at some bounded distance relative to each other. A fundamental concept in formation flying is the matching of the orbital energies of the deputy spacecraft with that of the chief. Recall that the purpose of this investigation is not to design the best formations for a particular mission; rather, the objective is to create a guidance strategy for a formation to achieve any desired geometry. Thus, the formation designs in the simulations highlight features of the guidance algorithm. The formation geometries ensure that the orbital energy matches across the formation members without additional requirements. The specific orbital energy for the chief is represented as Ec and, assuming a conic orbit, is evaluated from the chief orbit semi-major
axis, a_C: $E_c = -\mu/2a_c$. The specific energy associated with the orbit of a deputy is represented by E_d, and is defined as:

$$E_d = \frac{1}{2}\dot{r}_d^2 - \frac{\mu}{r_d} = \frac{1}{2}\left(\left(\dot{x} - \dot{\theta}_c y + \dot{r}_c\right)^2 + \left(\dot{y} + \dot{\theta}_c\left(x + r_c\right)\right)^2 + z^2\right) - \frac{\mu}{\sqrt{\left(x + r_c\right)^2 + y^2 + z^2}} \tag{5}$$

If these two energies are equated, the following relationship is produced:

$$\frac{1}{2}\left(\left(\dot{x} - \dot{\theta}_c y + \dot{r}_c\right)^2 + \left(\dot{y} + \dot{\theta}_c\left(x + r_c\right)\right)^2 + \dot{z}^2\right) - \frac{\mu}{\sqrt{\left(r_c + x\right)^2 + y^2 + z^2}} = -\frac{\mu}{2a_c} \tag{6}$$

Matching the orbital energies allows naturally bounded formations. For a given chief orbit, an initial deputy position, $\boldsymbol{\rho}$, is selected and the relative velocity values are determined from Equation 6. If the initial relative velocity is arbitrarily assumed in the $\hat{y}$-direction, periodic motion–that is, natural motion circumnavigation (NMC)–is produced as viewed in the Hill frame.

3.1.2 Relative Motion Approximations

There are numerous approximations for the relative motion of orbiting spacecraft, and the guidance algorithm exploits an approximation in the solutions to the delivery and assignment problems. The most well-known approximation is the Clohessy-Wiltshire (also labelled the Clohessy-Wiltshire-Hill or the Euler-Hill) equations–often abbreviated as "CW". The most typical formulation of the CW equations assumes a circular Chief orbit.[11] The state transition matrix (STM) that essentially maps the variations–i.e., position and velocity relative to the chief–in an initial state to variations downstream; application of the CW approximation yields an STM that is constant. The linear approximation employed for the relative motion dynamics in the guidance algorithm is expressed via the Yamanaka-Ankersen (YA) STM, one that does not assume a circular chief orbit.[12] Since the YA approximation applies to eccentric reference orbits, its region of applicability is much larger than the range that is valid for application of the CW equations. The trade-off is a more complex YA STM than the CW version since it requires information about the chief true anomaly for an accurately computation of the relative motion. Fortunately, evaluating the true anomaly along an orbit is accomplished iteratively for a conic using Kepler's equation. The YA STM is represented as $\Phi\left(t,t_0\right)$ and it is employed to propagate the relative position and velocity of a deputy spacecraft at time t_0 $\boldsymbol{\rho}_0$ and $\mathbf{v}_0$, forward in time:

$$\begin{bmatrix} \boldsymbol{\rho} \\ \mathbf{v} \end{bmatrix} = \Phi\left(t,t_0\right)\begin{bmatrix} \boldsymbol{\rho}_0 \\ \mathbf{v}_0 \end{bmatrix} \tag{7}$$

where $\boldsymbol{\rho}$ and $\mathbf{v}$ represent the relative position and velocity at time t, respectively. The YA STM is not constant, however the elements of $\Phi(t,\ t_0)$ are constructed analytically and numerical integration is not required for this approximation.[12]

3.1.3 Orbital Perturbations

The initial applications of the strategy to assign and deliver spacecraft in a formation occurs under the assumptions of Keplerian motion. Even in Earth orbit, however, spacecraft are subject to numerous forces including the gravitational effects of Earth oblateness, lunar gravity, solar gravity, atmospheric drag, and numerous smaller accelerations. To demonstrate the applicability of the approach to more complex dynamical models, an additional force is introduced in select simulations, i.e., Earth oblateness. To include such a force into the dynamical model, the numerical integration is accomplished in the Earth Centered Inertial (ECI) frame, although the formulation of the assignment and delivery problems remains in the Hill frame. Thus, for simulations that incorporate oblateness, the equations of orbital motion are perturbed by the Earth J_2 spherical harmonics. The dynamical equations are then rewritten as:

$$\ddot{\mathcal{X}} = -\frac{\mu \mathcal{X}}{r^3} - \frac{3}{2} J_2 \left(\frac{\mu}{r^2}\right)\left(\frac{R_e}{r}\right)^2 \left(1 - 5\left(\frac{\mathcal{Z}}{r}\right)^2\right)\frac{\mathcal{X}}{r} \tag{8}$$

$$\ddot{\mathcal{Y}} = -\frac{\mu \mathcal{Y}}{r^3} - \frac{3}{2} J_2 \left(\frac{\mu}{r^2}\right)\left(\frac{R_e}{r}\right)^2 \left(1 - 5\left(\frac{\mathcal{Z}}{r}\right)^2\right)\frac{\mathcal{Y}}{r} \tag{9}$$

$$\ddot{\mathcal{Z}} = -\frac{\mu \mathcal{Z}}{r^3} - \frac{3}{2} J_2 \left(\frac{\mu}{r^2}\right)\left(\frac{R_e}{r}\right)^2 \left(1 - 5\left(\frac{\mathcal{Z}}{r}\right)^2\right)\frac{\mathcal{Z}}{r} \tag{10}$$

where μ is once again the Earth's gravitational constant, R_e is the Earth equatorial radius, r is the orbital radius $r = \sqrt{\mathcal{X}^2 + \mathcal{Y}^2 + \mathcal{Z}^2}$, and $J_2 = 1082.63 \times 10^{-6}$ and is non-dimensional In these equations $\mathcal{X}$, $\mathcal{Y}$, and $\mathcal{Z}$ represent the ECI x, y, and z coordinates, respectively.

3.2 Delivery Problem

Once the spacecraft are assigned to their new positions in the formation, the task for the guidance algorithm is delivery of the spacecraft safely and efficiently to these new relative locations. In selecting a delivery approach, a key consideration is the balance between the total sum of the maneuvering ΔVs, the time of flight, and the computational demands. The introduction of the delivery methods occurs, however, prior to developing a framework for the assignment problem, because any decision process for assigning spacecraft to new positions is based on the guidance strategy to be employed for delivery. Two methods for solving the delivery problem are compared, i.e., artificial potential function (APF) guidance as well as model predictive control (MPC).

3.2.1 Artificial Potential Function Guidance

A guidance strategy employing artificial potential functions is an autonomous motion-planning methodology that links the kinematic planning problem with the dynamic execution problem in an efficient manner.[13, 14] This linkage is accomplished by creating a potential function that incorporates the necessary system information for the spacecraft to reach its goal: the minimum of the potential is placed at the target location and any obstacle locations are surrounded by areas of high potential. The consequence is a scheme such that the negative gradient of the potential leads to the desired target and avoids any obstacles. This gradient can represent the vehicle path; in this work, the negative gradient serves as the basis for the

design of the spacecraft maneuvers. The APF guidance strategy offers mathematical guidance laws that are implemented in real time and do not require any a priori assumptions concerning the system dynamics.[13, 14] The trade-off for this simplicity is an APF control law that is not inherently optimal. Consequently, the approach in this current analysis actually employs an extension of APF guidance denoted Adaptive Artificial Potential Function (AAPF) guidance. The AAPF guidance strategy employs state transition matrix representation of the system dynamics to adapt the potential field to the natural flow in the system in an effort to improve the propellant performance of the guidance system.[15]

The APF guidance scheme in the guidance algorithm is detailed in Wahl and Howell.[9] To create a potential field with the minimum value at the target and large values surrounding the obstacles, the potential function is separated into attractive and repulsive pieces. The attractive potential function is typically a Lyapunov candidate function to ensure that the spacecraft approaches the target asymptotically. The attractive potential, ϕ_a is a quadratic function based on the separation between the spacecraft position in the Hill frame, $\boldsymbol{\rho}$, and the target position in the Hill frame, $\boldsymbol{\rho}_t$. It is modeled as follows:

$$\phi_a = \frac{1}{2}\left(\boldsymbol{\rho}-\boldsymbol{\rho}_t\right)' Q\left(\boldsymbol{\rho}-\boldsymbol{\rho}_t\right) \tag{11}$$

This construction of ϕ_a ensures that the attractive potential is a Lyapunov function if the shaping matrix, Q, is positive-definite. In the adaptive artificial potential function approach, the matrix, Q, is 'shaped' to align with the natural flow in the relative motion dynamics. This information is available through the YA state transition matrix. Muñoz develops the shaping process.[9, 15] The companion component for APF guidance is the repulsive potential, ϕ_r. For N obstacles, define the repulsive potential as follows:

$$\phi_r = \frac{K}{2}\sum_{i=1}^{N}\frac{\left(\boldsymbol{\rho}-\boldsymbol{\rho}_t\right)' Q\left(\boldsymbol{\rho}-\boldsymbol{\rho}_t\right)}{\left(\boldsymbol{\rho}-\boldsymbol{\rho}_{o,i}\right)' P\left(\boldsymbol{\rho}-\boldsymbol{\rho}_{o,i}\right)-1} \tag{12}$$

Here, K is a constant scalar weighting factor and is determined by the user, $\boldsymbol{\rho}_{O,i}$ represents the position of the i-th obstacle in the Hill frame, and P is a positive-definite matrix that describes the size and shape of an ellipsoid. To structure the denominator in the repulsive potential, to create an ellipsoid of repulsion around each obstacle. This ellipsoid accommodates uncertainty in the obstacle position and shape. The numerator essentially includes the attractive potential to ensure that the target position is at the minimum of the total potential–similar to the method described by Ge and Cui as well as Muñoz.[15, 16] Tagging the other satellites as obstacles prevents intra-formation collisions, however, it is also possible to include obstacles beyond the formation members, e.g., debris or even other satellites.

To guide the spacecraft to the target location, the APF algorithm determines the relative velocity required at departure. The negative gradient of the total potential produces the desired velocity, $\mathbf{v}_d$, for the spacecraft to reach the target while avoiding collisions. The total potential is the sum of the attractive and repulsive portions: $\phi = \phi_a + \phi_r$. The desired velocity is then:

$$\mathbf{v}_d = -\nabla\phi = -\nabla\phi_a - \nabla\phi_r \tag{13}$$

This desired velocity vector, $\mathbf{v}_d$, as defined in the Hill frame and relative to the chief, guides the spacecraft to the target location—provided the target is stationary. To reach a moving target, the spacecraft must match both the target position and velocity to enable a rendezvous or to achieve the correct motion for the formation. The velocity matching is accomplished with a strategy similar to one used by Ge and Cui as well as Muñoz: a simple velocity matching condition that is added to the $\mathbf{v}_d$ computation.[15, 17]

To implement the velocity matching condition, combine the difference between the spacecraft and target velocities with the desired velocity from the negative gradient of the potential function. Additionally, a velocity-vector-angle-separation threshold serves as a check to determine if a maneuver is necessary. The velocity vector for the spacecraft, in terms of the Hill frame, is represented by $\mathbf{v}$ and the target velocity vector by $\mathbf{v}_t$, where the components are defined:

$$\mathbf{v} = \begin{bmatrix} \dot{x} & \dot{y} & \dot{z} \end{bmatrix}^T \tag{14}$$

An error in velocity, $\boldsymbol{\varepsilon}_{\mathrm{v}}$, is defined as the difference between the spacecraft and target velocity vectors:

$$\boldsymbol{\varepsilon}_{\mathrm{v}} = \mathbf{v} - \mathbf{v}_t \tag{15}$$

The angle, ψ, between $\boldsymbol{\varepsilon}_{\mathrm{v}}$ and $\mathbf{v}_d$ is also defined:

$$\psi = \arccos\left(\frac{\boldsymbol{\varepsilon}_{\mathrm{v}} \cdot \mathbf{v}_d}{|\mathbf{v}_d||\boldsymbol{\varepsilon}_{\mathrm{v}}|} \right) \tag{16}$$

If ψ is larger than a user-defined threshold, ψ^*, then the APF guidance strategy recommends an impulsive maneuver, $\Delta\mathbf{V}$, defined as the difference between $\mathbf{v}_d$ and $\boldsymbol{\varepsilon}_{\mathrm{v}}$:

$$\Delta\mathbf{V} = \mathbf{v}_d - \boldsymbol{\varepsilon}_{\mathrm{v}} \tag{17}$$

Again, express this impulsive $\Delta\mathbf{V}$ in terms of Hill frame coordinates and define it relative to the chief. In this investigation, a threshold angle such that, $\psi^* = 45^o$, is incorporated throughout the analysis.

For efficiency, any maneuver recommended by the guidance law should be feasible to accomplish. Since artificial potential function guidance and, to a lesser extent, adaptive artificial potential function guidance uses the distance between the spacecraft and target as the basis for determining the size of the recommended maneuvers, APF and AAPF can both recommend $\Delta\mathbf{V}$ values that are not feasible for actual implementation. Incorporating an approximation to the natural dynamics in the AAPF computations reduces this effect, but may not eliminate it in every scenario. Capping the size of individual maneuvers in the simulations bounds the available impulsive $\Delta\mathbf{V}$ magnitude, ΔV, via an upper limit. For the simulations here, each impulsive ΔV ΔV is capped at 0.5 m/sec. Thus, at this time, the total ΔV along a trajectory is not limited, but each impulsive maneuver is bounded by 0.5 m/sec. Conversely, there is no lower bound on ΔV; such a lower bound can be incorporated.

Some parameters in the APF structure are straightforward to tune. These include K, P , and the look-ahead time, τ . The look-ahead time determines the forward propagation time for the YA STM, which is then used to create the attractive potential, φ_a.[9] The selection for the look-ahead time,τ , impacts the performance of the APF guidance algorithm; however, thus far, the investigation has not revealed a consistent "best" choice for the value of τ . For the simulations in this investigation, unless otherwise noted, a constant τ value equal to one-fourth of the chief orbital period is consistently applied. This value for τ incorporates sufficient relative motion information to plan useful maneuvers but does not adversely affect the computational time. The other two parameters influence the repulsive potential, φ_r, and, in this investigation, unless otherwise noted, K is assigned a value of 1/20, and P is fixed to equal
$P = \left(1 \diagup 25^2 \right) \times I_{3\times 3}$. This selection for P creates a sphere of repulsion with a 25-m radius, i.e., obstacles of substantial size. This value of K delivers reliable obstacle avoidance while not recommending unnecessarily large maneuvers.

3.2.2 Model Predictive Control Algorithm

Artificial potential function guidance possesses advantages and disadvantages. The main advantages include its computational simplicity that enables on-board operation and its inherent obstacle avoidance capability that prevents collisions. The main disadvantage of an

APF guidance strategy is the inefficient use of maneuvers. While an adaptive artificial potential function alteration mitigates these inefficiencies, an alternative guidance approach may yield more propellant-efficient trajectories. Thus, a model predictive control (MPC) strategy as an alternative approach is explored for solving the delivery problem and to serve as a comparison for maneuver efficiency. Model predictive control (MPC) is an optimization-based control strategy that is structured and implemented in numerous ways. To enable a reduction in the computational load and delivery of a guidance algorithm more amenable to on-board implementation, the optimization of the cost function is recast as a quadratic programming problem as described by Brand et al.[18] The approach requires a linear model of the dynamics and, for this investigation, the Yamanaka-Ankersen state transition matrix is employed to approximate the relative motion dynamics.[12] Recasting the optimization of the MPC cost function as a quadratic programming problem offers a more efficient solution process, for example, using the interior-point and active-set methods described by Wright.[19] However, one of the disadvantages of using quadratic programming to solve the optimization problem is its requirement for linear inequality constraints. Obstacles, e.g., other spacecraft or general debris, represent nonlinear constraints on the spacecraft trajectory–to avoid collisions. To overcome the problem of collisions requires the introduction of two additional steps. The first is establishing ellipsoidal path constraints about any obstacles in a manner similar to Jewison et al.[20] These nonlinear constraints violate the parameters of a quadratic problem, so a nonlinear optimization method–like sequential quadratic programming–is now required. The second step is the inclusion of an element in the cost function that seeks to maximize the separation between the spacecraft and any obstacles.

3.2.2.1 Objective Function Design

Model predictive control is essentially a receding horizon approach to compute a future control profile that optimizes an open-loop performance objective. Over a number of future time-steps, N , a series of control inputs, $\mathbf{u}_i$, are computed such that a cost function is minimized; subsequently, only the first control input is implemented and, at the next time step, the process repeats with the computation of a new series of $\mathbf{u}_i$. A type of feedback loop is implemented such that the positions and velocities for both the spacecraft and target are updated and as the future control inputs are reconstructed at each step. As previously noted, the dynamic model incorporated into the MPC guidance scheme is linear. The model for the linear dynamics:

$$\mathbf{x}_{k+1} = \Phi\left(t_{k+1}, t_k\right)\left(\mathbf{x}_k + B\mathbf{u}_k\right) \tag{18}$$

where $\mathbf{x}_k$ is the state of the spacecraft as observed in the Hill frame, $\mathbf{x} = [\boldsymbol{\rho},\ \mathbf{v}]^T$ at time t_k, $\mathbf{u}$ represents the impulsive ΔV maneuver, $\Phi(t_{k+1}, t_k)$ is the YA STM from time t_k to t_{k+1}. The control matrix, B, is defined as: $B = \begin{bmatrix} 0_{3\times3} & I_{3\times3} \end{bmatrix}$. This formulation does allow the incorporation of the Yamanaka-Ankersen state transition matrix, not as a constant matrix, but one that evolves with time.

The objective function for minimization is based on the quadratic difference between the spacecraft state at each time step, $\mathbf{x}_k$ and the target state at the final time step (originating from time step k), $\mathbf{x}_k^*$ and a quadratic function of the control cost at each time step, $\mathbf{u}_k$. The optimization problem as characterized:

$$\min_{\mathbf{U}_k} \mathcal{J}(\mathbf{U}_k, \mathbf{x}_k) \tag{19}$$

where $\mathbf{U}_k$ is a stacked vector of the control vectors, $\mathbf{U}_k = \left[\mathbf{u}_k, \mathsf{K}, \mathbf{u}_{k+\mathcal{N}-1}\right]^T$, and the objective function, J, is a balance between the deviations and the control effort: $\mathcal{J}(\mathbf{U}_k, \mathbf{x}_k) = \mathcal{J}_1(\mathbf{x}_k) + \mathcal{J}_2(\mathbf{U}_k)$. The first component, $\mathcal{J}_1$, addresses the state differences:

$$\mathcal{J}_1(\mathbf{x}_k) = \left(\mathbf{x}_{k+\mathcal{N}} - \mathbf{x}_k^*\right)^T \bar{S} \left(\mathbf{x}_{k+\mathcal{N}} - \mathbf{x}_k^*\right) + \sum_{i=}^{\mathcal{N}-1} \left(\mathbf{x}_{k+i} - \mathbf{x}_k^*\right)^T S \left(\mathbf{x}_{k+i} - \mathbf{x}_k^*\right) \tag{20}$$

where S is the weighting (or penalty) matrix on the difference in the six-dimensional state for all but the final time step; then, the matrix $\bar{S}$ is the weighting on the final time step. In the operational guidance algorithm, the weights are assigned values such that $S = 10^{-10} I_{6\times6}$,where I is the identity matrix. The weighting on the final state variation, $\bar{S}$ is formed from the discrete-time algebraic Riccati equation, i.e.:

$$\begin{aligned} \bar{S} &= \Phi(t_{k+\mathcal{N}}, t_k)^T \bar{S} \Phi(t_{k+\mathcal{N}}, t_k) + S^* - H^T \left(\mathcal{R} + B^T \bar{S} B\right) H \\ H &= \left(\mathcal{R} + B^T \bar{S} B\right)^{-1} B^T \bar{S} \Phi(t_{k+\mathcal{N}}, t_k) \end{aligned} \tag{21}$$

where S^* functions as an initial value for $\bar{S}$, with a value such that $S^* = 10^{-1} I_{6\times6}$. Note that $\mathcal{R}$ is also a weighting matrix on the control cost. Prior to every time step, the discrete-time algebraic Riccati equation is solved for $\bar{S}$, but this computation is efficiently accomplished with a numerical algorithm. The second component of $\mathcal{J}$ is then defined:

$$\mathcal{J}_2\left(\mathbf{U}_k\right) = \sum_{i=0}^{\mathcal{N}-1} \mathbf{u}_{k+i}^T \mathcal{R} \mathbf{u}_{k+i} \tag{22}$$

where $\mathcal{R}$ is the weighting on the control cost, which also appears in Equation 21, and is equal to $\mathcal{R} = 2\times10^4\ I_{3\times3}$. These values of $\mathcal{R}$, S^* and S, and the large differences between them, are selected to prioritize the minimization of ΔV rather than the minimization of the difference in spacecraft-target state vectors, while still delivering the spacecraft to the target.

3.2.2.2 Quadratic Program Formulation

The optimization problem as defined in Section 3.1 in Equation 19 can be recast as a quadratic programming problem in a manner described by Brand et al.[18] Recasting the optimization problem as a quadratic programming problem allows a solution with a fast numerical algorithms–thus, easing the computational burden on the spacecraft processes. This quadratic programming problem is written in the form:

$$\begin{aligned} &\min_{\mathbf{U}_k}\left(\frac{1}{2}\mathbf{U}_k^T \mathcal{Q} \mathbf{U}_k + \mathcal{H}^T \mathbf{U}_k\right) \\ &\mathcal{V}\mathbf{U}_k \le \mathcal{W} \end{aligned} \tag{23}$$

The matrices $\mathcal{Q}$ and $\mathcal{H}$ are produced from combinations of the weighting matrices $\mathcal{R}$, $\bar{S}$, and S, the control matrix, B, and the YA STM, $\Phi\left(t_{k+1}, t_k\right)$; the constraint matrices $\mathcal{V}$ and $\mathcal{W}$ are then produced from any path or control constraints input by the user. The details for the construction of these matrices appear in Brand et al.[18] The time varying nature of the Yamanaka-Ankersen STM requires a slight modification of the linear system representation, but this change is accomplished in Equation 18. Despite easing the computational burden over the optimization process, the quadratic program formulation is limited to only linear constraints–the $\mathcal{V}$ and $\mathcal{W}$ matrices. Obstacles viewed in the relative motion frame present non-linear constraints along the path, which must be avoided to prevent collisions.

3.2.2.3 Obstacle Avoidance

One of the necessary features in any autonomous solution to the delivery problem is the successful avoidance of collisions between the spacecraft in the formation and other obstacles. An inherent advantage exists in favor of artificial potential function guidance since obstacle avoidance is a fundamental APF characteristic with the inclusion of a repulsive potential.

Formulation of the optimization step in a model predictive control scheme as a quadratic programming problem greatly reduces the computational burden on an optimizer but, to successfully avoid collisions, the strict quadratic programming structure is abandoned in this implementation. Robust obstacle avoidance in the MPC guidance system is incorporated in two alternate steps. First, in a method similar to one described by Jewison et al.,[20] the MPC optimization problem is solved with a constrained non-linear optimization algorithm, in this application. sequential quadratic programming (SQP), with ellipsoidal path constraints surrounding every obstacle. The second step is the inclusion of a third element in the cost function in Equation 19, such that an additional penalty is introduced as the spacecraft approaches any obstacle; the inclusion of this element is motivated by previous experience with APF guidance and its success in collision avoidance.

To create the constraints for the model predictive control path, the motion of the spacecraft and any obstacles are also modeled over a series of time-steps. Similar to creating the path of the spacecraft through the stacked control vector, $\mathbf{U}_k$, and the YA STM, the paths of any obstacles are also modeled with the same linear approximation. The state corresponding to an obstacle at time t_k in the Hill frame is represented as $\mathbf{x}_{o,k}$, and the obstacles are assumed to move only with the natural dynamics–i.e., they do not introduce any maneuvers. Depending on the length of the time steps, it may be necessary to interpolate between the time steps to properly avoid collisions; for example, the time steps in the cost function are nominally 5 minutes apart but potential collisions may occur between the 5 minute measurements. Interpolation adds numerous elements to the constraint function–adding to the computational load. To offset this increase, the constraint computations over the time steps are not fully activated. Over the total number interpolated steps, an inequality constraint must be satisfied for every step i:

$$c(i) = 1 - \left(\boldsymbol{\rho}_i - \boldsymbol{\rho}_{o,i}\right)^T P \left(\boldsymbol{\rho}_i - \boldsymbol{\rho}_{o,i}\right) < 0 \tag{24}$$

where $\boldsymbol{\rho}_i$ and $\boldsymbol{\rho}_{O,i}$ represent the position of the spacecraft and obstacle relative to the Chief in the Hill frame at step i. The matrix P is the same quantity that appears in the APF guidance method that serves to define an ellipsoid surrounding every obstacle. This constraint is applied for every obstacle, which, at a minimum, includes the other spacecraft in the formation.

The second step incorporated to avoid obstacles is the addition of an element to the objective function. Thus, the cost function includes a third term, i.e., $\mathcal{J} = \mathcal{J}_1 + \mathcal{J}_2 + \mathcal{J}_3$. The new addition, $\mathcal{J}_3$, is structured similarly to the repulsive potential, ϕ_r, from the APF guidance scheme. For N obstacles and $\mathcal{N}$ time steps:

$$\mathcal{J}_3 = \mathcal{K} \sum_{j=1}^{N} \sum_{i=1}^{\mathcal{N}} \frac{1}{\left(\left(\boldsymbol{\rho}_{k+i} - \boldsymbol{\rho}_{oj,k+i} \right)^T P \left(\boldsymbol{\rho}_{k+i} - \boldsymbol{\rho}_{oj,k+i} \right) - 1 \right)^2} \tag{25}$$

where $\boldsymbol{\rho}_i$ is the position of the spacecraft at step i and $\boldsymbol{\rho}_{O,j,i}$ is the position of the j-th obstacle at step i. An ellipsoidal boundary–of size and shape determined by P –is established around each obstacle. Once again, P is the same matrix that appears in the APF delivery scheme. The weighting on $\mathcal{J}_3$ is $\mathcal{K}$, which is not the same weighting, K, used in ϕ_r, and is selected to be sufficiently large to influence the path away from obstacles, but not so large as to prevent reaching the target.

3.2.3 Demonstrations

A demonstration of the MPC guidance strategy appears in Figure 2(a). For this first simulation, there are no obstacles present. The spacecraft initial position is highlighted by the red circle, and the initial path is the green dashed line. The target trajectory is plotted in blue, and the spacecraft trajectory in red. The final position of the spacecraft is represented as a red square, while the target appears as a blue asterisk. The black arrows indicate the initial direction of motion, while the colored arrows represent the location and direction of maneuver ΔV s. For this simulation, the chief orbit is characterized by a perigee altitude of 1,276 km and an eccentricity of 0.125. The MPC guidance scheme uses the previously described values for $\bar{S}$, S, and $\mathcal{R}$. Each time step is 5 minutes, and the guidance looks ahead for $\mathcal{N}$ = 11 time steps. The MPC guidance scheme uses 0.48 m/s of maneuvering ΔV and requires 180 minutes to complete the maneuver. A demonstration of the MPC performance in the presence of obstacles is demonstrated in Figure 2(b). The chief orbit and the initial conditions for the spacecraft and target are identical to the previous example. An obstacle, a sphere of radius 25 m, is added with an initial position and velocity defined to intercept the spacecraft trajectory

from Figure 2(a). The colored spheres indicate the position of the obstacle at each time step, with the green shading representing the beginning of the simulation evolving to red later in the simulation. The MPC cost function includes $\mathcal{K}$ = 100 in $\mathcal{J}_3$, and the collision constraint, described in Equation 24, is applied over the first two look ahead time steps with an interpolation every 20 seconds. The MPC guidance strategy consumes 0.52 m/s of maneuvering ΔV and, again, uses 180 minutes to complete this maneuver.

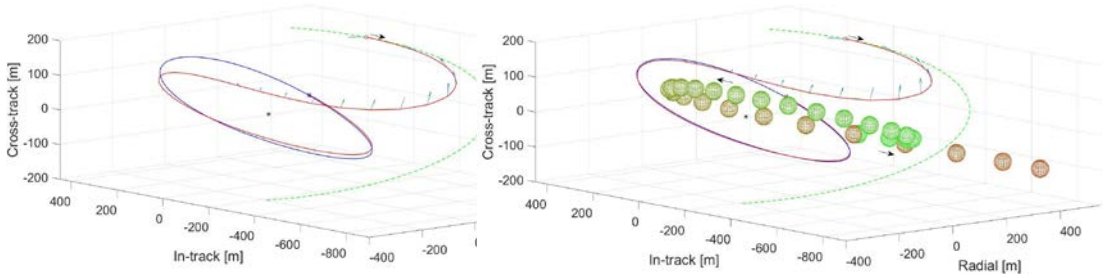

(a) No obstacles. (b) Moving obstacle.

Figure 2. Demonstration of MPC Guidance

3.3 Auction Algorithm

The assignment problem is formulated as the task of assigning spacecraft to new positions in the formation; consequently, n spacecraft must be matched to n targets in the desired formation. A quantifiable cost, b_{ij}, is associated with the matching of each spacecraft i to target j, and the goal is the assignment that minimizes the total cost to the entire formation. This construction of the assignment problem is known as a "linear sum assignment problem" and there are numerous approaches to solving such problems, each with advantages and disadvantages.[8] As previously discussed, the overarching guidance scheme employs an auction process (also labelled an "auction algorithm") to assign the spacecraft; the auction algorithm is attractive because of its computational simplicity, its success in producing near-equilibrium (minimized cost) assignments,[7] and its ability to be implemented in parallel.[21, 22]

In Wahl and Howell,[9] the auction process is based on the strategy of Bertsekas and involves preassigning the targets to spacecraft before initiating the auction algorithm proper.[7] In certain cases, this initialization of the algorithm biases the result of the auction process so that the result is no longer the "best" assignment for the formation. This defect is corrected via an improved auction process also based on the framework of Bertsekas.[23] The main difference with the improved version is a step that separates each auction round into a bidding phase and an assignment phase, thus eliminating the initialization bias and adding extra functionality to the auction procedure.

3.3.1 Cost, Price, Expense, and Satisfaction

A key to a successful auction is determining the costs associated with each spacecraft target pairing such that the final assignment corresponds to a desirable formation from the operator viewpoint. The costs used in the auction are based on the estimated ΔV, the estimated time of flight (ToF), or some suitable combination. Before the auction commences, the algorithm first determines the cost values for each spacecraft to reach every target. These estimates are produced via running a simulation of the spacecraft traveling to every target using the YA STM to represent the relative motion dynamics and either the APF or MPC (depending on which approach is used during the computation of the maneuver) guidance strategy to deliver the spacecraft. In these cost calculation simulations, no obstacles are incorporated, and, in the MPC case, the quadratic-programming formulation computes the control costs. For example, for spacecraft i traveling to target j, the maneuvering ΔV in the simulation is ΔV_{ij} in units of m/s and time required is ToF_{ij} in units of the chief orbital period. These are combined to yield the cost of target j for spacecraft i such that:

$$b_{ij} = \Delta V_{ij}^{F} \; ToF_{ij}^{L} \tag{26}$$

where F and L are the scalar weightings on maneuvering cost and time of flight, respectively. In a more sophisticated strategy, the weightings can be separated by spacecraft, Fi and Li, by target, F_j and L_j, or some combination of the two. In the examples here, the values of F and L are always either 1 or 0, such that if $F = 1$ then $L = 0$ and vice versa; thus, the cost is based solely on ΔV or ToF.

Separate from the cost assessed for every pairing, each target also commands its own price. The prices can be initially set to the same value over all targets, or the prices can be set individually. For target j, the price is denoted p_j. As the auction proceeds, the prices may rise, and the desirability of the targets are modified. The expense of target j to spacecraft i is represented by v_{ij} and is the combination of cost and price, i.e.:

$$v_{ij} = b_{ij} + p_j \tag{27}$$

In the auction, each spacecraft is seeking to minimize its expense. Spacecraft i is "satisfied" with target j if:

$$v_{ij} = \min_{k=1,\mathrm{K},n} \{v_{ik}\} + \varepsilon \tag{28}$$

where ε is a slack variable introduced to prevent tie bids and to speed up the auction process– this technique is labeled as "ε-Complementary Slackness."[7] An "equilibrium assignment" occurs when all spacecraft are satisfied. Bertsekas investigates the optimal size for ε and determines that, for n members of the auction, the optimal size is $\varepsilon < 1/n$.[7] In the auction algorithm incorporated into the guidance strategy, $\varepsilon = 1/(n+1)$. As the number of spacecraft, n, increases, ε decreases.

3.3.2 Bidding Phase

Once all the costs are computed for every spacecraft, the auction begins. In the beginning, all the spacecraft are unassigned, and, as the auction proceeds, spacecraft are gradually assigned until the auction terminates with every spacecraft assigned to a target. Each round of the auction starts with the bidding phase and only unassigned spacecraft participate in the bidding phase. Let I indicate the subset of unassigned spacecraft. Then for each spacecraft i, where $i \in I$, the algorithm determines the target, j_i, with the minimum expense for spacecraft i:

$$j_i = \operatorname{arcmin}_{j \in A(i)} \{v_{ik}\} \tag{29}$$

where $A(i)$ is the subset of targets that are available to spacecraft i. For the following simulations, every target is available to every spacecraft, so $A(i) = 1, \ldots, n$. However, this auction formulation allows for scenarios where certain spacecraft are restricted to subsets of the targets. With the most desirable target identified, the corresponding minimum expense, v_i, is also constructed:

$$v_i = v_{ij_i} = b_{ij_i} + p_{j_i} = \min_{j \in A(i)} \{v_{ij}\} \tag{30}$$

The second lowest expense, ω_i is also evaluated:

$$\omega_i = \min_{j \in A(i), j \neq j_i} \{v_{ij}\} \tag{31}$$

With the lowest, v_i, and second lowest, ω_i, set of expenses determined, spacecraft i will create a bid, γ_i, for target ji, one that is based on the difference between the minimum and second lowest expense such that:

$$\gamma_i = \omega_i - v_i + \varepsilon \tag{32}$$

where the slack variable, ε, once again emerges to ensure that the minimum bid size is ε Every unassigned spacecraft is processed and submits a bid. It is possible that one target receives multiple bids and several targets receive no bids. The auction algorithm records which targets received bids, the bid values, and the spacecraft bidding. The auction then moves into the assignment phase.

3.3.3 Assignment Phase

In the assignment phase, every target that received a bid follows up with a procedure to be assigned a spacecraft. For target j, let $\Pi(j)$ be the set of spacecraft submitting bids. First, the algorithm identifies the bidder, ij, with the highest bid:

$$i_j = \operatorname{argmax}_{i \in \Pi(j)} \{\gamma_i\} \tag{33}$$

The corresponding maximum bid, γ^*, is determined:

$$\gamma^* = \max_{i \in \Pi(j)} \{\gamma_i\} \tag{34}$$

Next, target j is assigned to spacecraft i_j and target j's price, p_j, increases by γ^*:

$$p_j^+ = p_j^- + \gamma^* \tag{35}$$

where p_j^- represents the prior price and p_j^+ represents the price after the bid is added. Any spacecraft that was previously assigned to target j is now unassigned, and any other spacecraft in $\Pi(j)$ remain unassigned. Once every target that received a bid goes through this procedure and the prices are accordingly adjusted, the algorithm returns to the bidding phase and the process repeats if any spacecraft remain unassigned. The auction terminates once every spacecraft is assigned, and that assignment is then used in the delivery phase of the guidance algorithm. The improved auction structure allows for scenarios with an unequal number of spacecraft and targets, perhaps representing a formation that has lost one or more spacecraft.

3.3.4 Demonstration

A demonstration of the improved auction process begins with the formation as illustrated in Figure 3. The chief orbit for this scenario is characterized by a perigee altitude of 1,000 km and an eccentricity of 0.1; the chief location in the Hill frame is depicted as a black asterisk. The initial positions of the spacecraft (corresponding to the chief perigee) are denoted as red circles and numbered 1 through 4. The initial positions of the targets in the desired formation are depicted as blue circles and identified as *A* through *D*, their trajectories are represented in blue with arrows indicating the direction of motion. For this simulation, the auction employs the APF guidance scheme to compute the costs. Additionally, the costs are solely evaluated from the estimated ΔV, so $F = 1$ and $L = 0$ in Equation 26. The costs corresponding to each pairing are summarized in Table 1. Initially, all the targets are assigned the same price, i.e., zero.

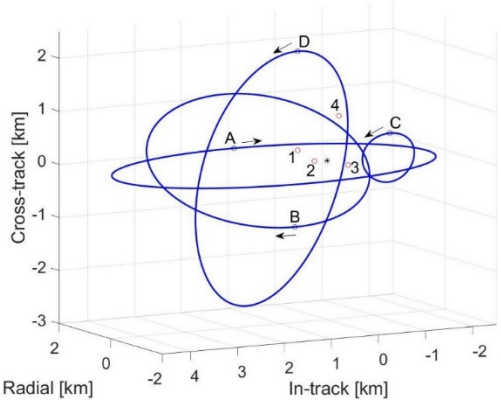

Figure 3. Auction Example

Spacecraft Initial Positions Depicted as Red Circles, the Target Trajectories in Blue, the Chief Pint as a Black Asterisk, and Target Initial Positions as blur Circles. Arrows Indicate the Direction of Motion

With the costs for each pairing tabulated, the auction begins. Evident in Table 1, target *C* possesses the lowest cost for each spacecraft and, therefore, receives bids from all four spacecraft. In the first round, spacecraft 4 offers the largest bid, thus, it is assigned to target *C*, and the price for target *C* is increased. Since spacecraft 1 through 3 are still unassigned, the auction continues. For this scenario, the auction terminates after seven rounds–when all spacecraft are assigned to targets. The final price for each target is listed in Table 2; clearly, the highest price occurs for target *C*–corresponding to its desirability–and target *D* earns the lowest price–corresponding to its high cost for every spacecraft.

The measure for an assignment is defined as the satisfaction as described in Equation 28. A summary reflecting the final assignment of each spacecraft (*S/C*) appears in Table 3. For each spacecraft, the final assignment (*Tar*), the corresponding expense (*Exp*), the minimum expense (Exp^*), and the corresponding desired target (Tar^*) are included. There are two spacecraft (3 and 4) that are not assigned to their most desired target (*A* and *C,* respectively). However, these spacecraft are within ε of their minimum expenses, demonstrating that these spacecraft are "satisfied" with the assignment. (For four

Table 1. Pairing Costs for Figure 3 (Unit-less)

	A	***B***	***C***	***D***
1	1.5147	4.0046	0.7919	4.2242
2	2.4462	2.7876	1.8264	4.0153
3	1.6945	3.2936	1.1334	5.2550
4	2.1595	4.4362	0.9358	3.3961

Table 2: Final Prices for Targets in Figure 3

	A	***B***	***C***	***D***
p	1.9634	0.6625	2.7245	0.4643

Table 3. Final Assignment and Expenses for Figure 3

S/C	***Tar***	***Exp***	***Exp****	***Tar****
1	*A B*	3.4781	3.4781	*A B*
2	*C D*	3.4501	3.4501	*A C*
3		3.8579	3.6579	
4		3.8603	3.6603	

spacecraft $\varepsilon = 1/5$.) The auction process succeeds in producing satisfactory assignments for the formation.

4 RESULTS AND DISCUSSION

The performance of the complete guidance algorithm is analyzed through maneuver simulations in several formation reconfiguration scenarios. The differences between the performance of the APF and the MPC delivery options are noted. The initial scenario (Pentagon Reconfiguration) involves a 5-spacecraft formation with a chief orbit perigee altitude of 1,000 km and eccentricity of 0.1. In this formation, the chief location is actually unoccupied by any spacecraft and exists only as a reference point. The initial state for this scenario is displayed in Figure 4, where the spacecraft initial positions are represented as red circles, and the target formation appears in blue. The spacecraft are numbered 1- 5 and the targets are *A* - *E*. For the following simulations, no additional obstacles are included; that is, the spacecraft are only avoiding intra-formation collisions.

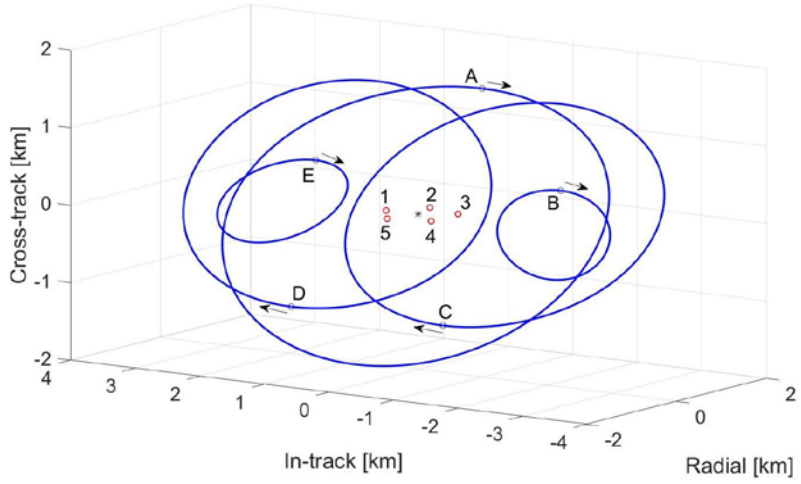

Figure 4. Pentagon Reconfiguration Spacecraft Initial Positions

The Pentagon reconfiguration spacecraft initial positions are depicted as the Red Circles, the Target Trajectories in Blue, the Chief Point as a Black Asterisk, and Target Initial Positions as Blue Circles. Arrows Indicate the Direction of Motion

Four simulations are presented for this starting scenario. Each delivery method, MPC and APF, is tested and each auction cost computation, i.e., all ΔV or all ToF is employed. The internal parameters for each delivery method are described previously, except for $\mathcal{K}$ in Equation 25—which is set equal to 0.2. Unless otherwise noted, all simulation dynamics assume a spherically symmetric Earth. The results from the simulations appear in Table 4, where the Delivery Method "DM" column indicated the delivery method, "Auc" reflects the auction cost evaluations approach, underneath each "*S/C*" is the spacecraft assignment, "ΔV" lists the total formation maneuvering ΔV, and "Time" is the time interval required for all the reconfiguration maneuvers. For this scenario, the MPC delivery method produces maneuvers that use less ΔV when compared to the APF method, and–conversely–the APF method offers much shorter times of flight. This result is not surprising since the MPC method is built around optimizing control usage. The different auction cost computation approaches do not result in a significant difference as the delivery schemes, however, there is an effect. For MPC delivery, there is no difference in the time of flight; the resulting ΔV values are different, however, with the lower ΔV value emerging from the auction using estimated ΔV in its cost calculations. For APF delivery, the results conform to expectations. The assignment based on ToF yields a lower time of flight, and the assignment based on ΔV produces a lower total control cost. The formation maneuver with MPC delivery and ΔV auction weighting is plotted in Figure 5(a) and the formation maneuver with APF delivery and ToF auction weighting is shown in Figure 5(b). Clearly, the differences in the paths are evident.

Table 4. Guidance Comparison Results for Figure 4

DM	**Auc**	***S/C* 1**	***S/C* 2**	***S/C* 3**	***S/C* 4**	***S/C* 5**	**ΔV [m/s]**	**Time [min]**
MPC	ΔV	*E D*	*A A*	*B B*	*C E*	*D C*	8.05	300
MPC	*ToF*	*D C*	*A B*	*B A*	*C D*	*E E*	8.39	300
APF	ΔV						10.13	142.5
APF	*ToF*						10.82	138

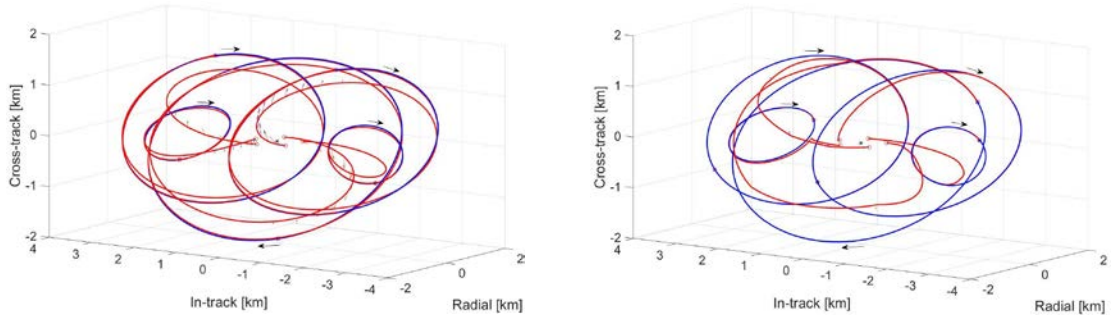

(a) MPC Formation Guidance **(b) APF Formation Guidance**

Figure 5. Pentagon Reconfiguration Spacecraft Trajectories

The pentagon reconfigure spacecraft trajectories are in red, Target Trajectories in Blue. Colored Arrows Indicate the Direction and Location of Impulsive Maneuvers, Black Arrows Indicate Direction of Motion

The second scenario (Tetrahedron Deployment) involves a simulated deployment maneuver. The four spacecraft originate close to the chief location and then move to a formation selected to form a tetrahedron at the chief orbit perigee. The chief orbit has a perigee altitude of 3,189 km and eccentricity of 0.15. The scenario starting conditions are displayed in Figure 6, where the spacecraft initial positions are denoted by red circles, and the target formation trajectories are in blue with the positions at perigee represented by blue circles. The initial–that is, before any maneuvers are performed–trajectories of the spacecraft are in red as well. The spacecraft are numbered 1- 4 and the targets are *A* - *D*. Once again, no extra-formation obstacles are included in the simulations.

Again, four simulations are presented for this deployment scenario. Each delivery method, MPC and APF, is tested with each auction cost computation approach, all ΔV or all *ToF*. The internal parameters for each delivery method are the same as in the previous example, and the simulation dynamics again assume a spherically symmetric Earth. The results for the simulations are presented in Table 5. There is a surprising result that the MPC delivery method does not give the lowest ΔV maneuvers. The APF delivery with ΔV auction weighting gives the lowest, followed by the two MPC simulations, and then the other APF simulation. Once again, the MPC simulations have the same time of flight, but the ΔV weighted auction does have a lower maneuver cost. The APF simulations behave as expected, with the *ToF* auction weighting delivering a shorter time of flight, but higher ΔV cost. The formation maneuver with MPC delivery and *ToF* auction weighting is plotted in Figure 7(a) and the formation maneuver with APF delivery and ΔV auction weighting is shown in Figure 7(b).

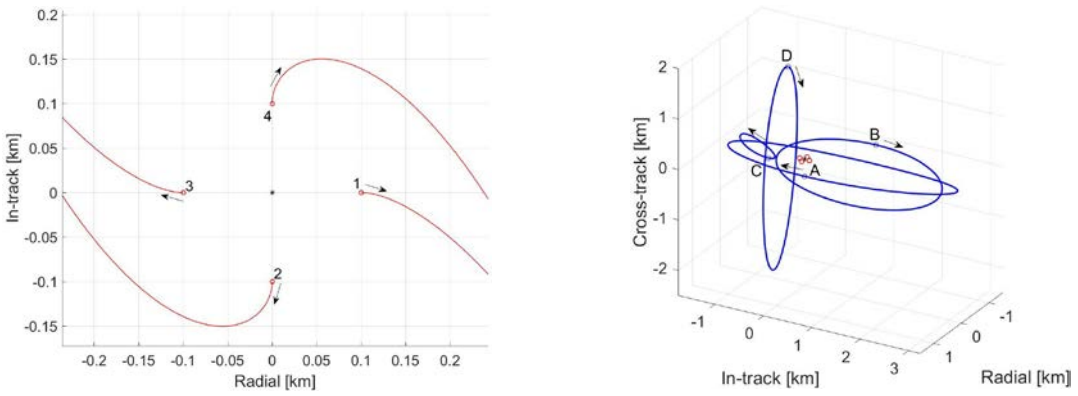

(a) Spacecraft Initial Positions and Trajectories **(b) Target Formation**

Figure 6. Tetrahedron Deployment. Spacecraft Initial Positions

Can be shown depicted as Red Circles, the Target Trajectories in Blue, the Chief Point as a Black Asterisk, and Target Initial Positions as Blue Circles. Arrows Indicate the Direction of Motion

Table 5. Guidance Comparison Results for Figure 6

DM	Auc	S/C 1	S/C 2	S/C 3	S/C 4	ΔV [m/s]	Time [min]
MPC	ΔV	C A	A C	B D	D B	4.09	220
MPC	oF	C B	A D	B A	D C	4.36	220
APF	ΔV					3.66	185
APF	oF					5.29	118.5

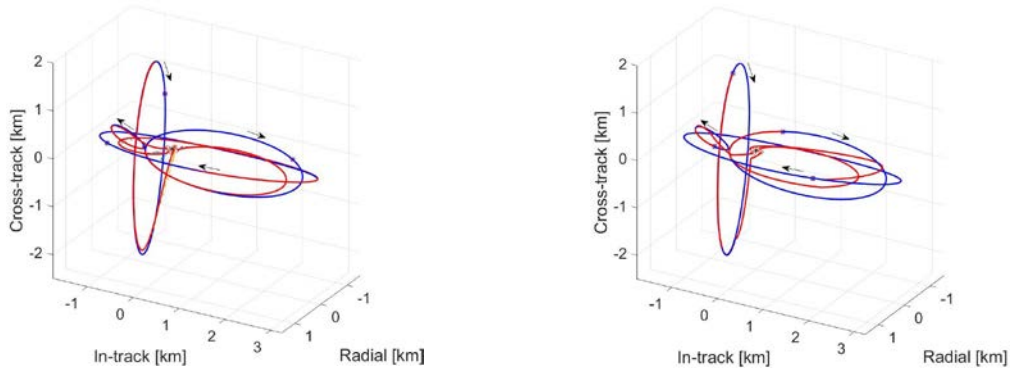

(a) MPC Formation Guidance **(b) APF Formation Guidance**

Figure 7. Tetrahedron Deployment. Spacecraft Trajectories

Are shown in Red, Target Trajectories in Blue. Colored Arrows Indicate the Direction and Location of Impulsive Maneuvers, Black Arrows Indicate Direction of Motion

For the final scenario (J_2 Deployment), the simulations take place under dynamics perturbed by Earth J_2 spherical harmonic and utilizing Equations 8 - 10. The chief orbit for this simulation once again has a perigee altitude of 1,000 km, eccentricity of 0.1, and an inclination of 10 degrees. The scenario is once again a deployment maneuver for a 4-spacecraft formation, and the spacecraft starts at similar locations as in Figure 6(a); however, the target formation is different. The target formation and initial spacecraft positions are displayed in Figure 8, with the targets labeled *A* through *D*.

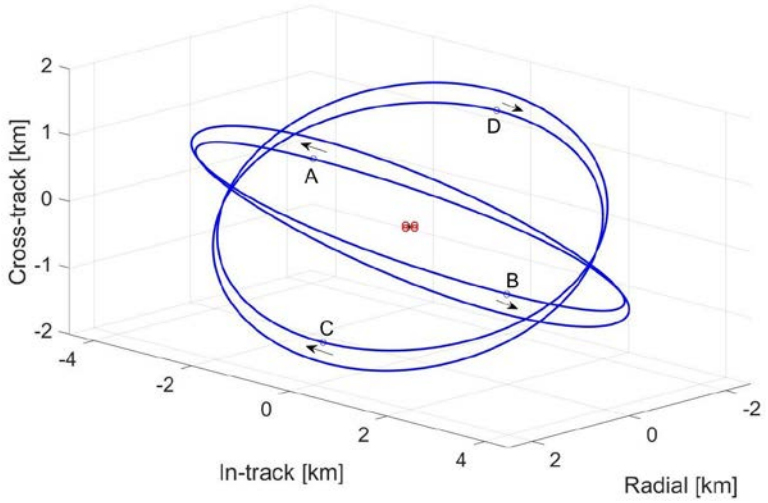

Figure 8. J_2. Deployment Spacecraft Initial Positions

As shown in the figure above J_2 deployment spacecraft initial positions are the Red Circles, the Target Trajectories in Blue, the Chief Point as a Black Asterisk, and Target Initial Positions as Blue Circles. Arrows Indicate the Direction of Motion

The first simulation for this scenario uses the MPC guidance scheme to deliver the spacecraft and the auction algorithm with ΔV weighting to assign the targets to spacecraft. The full maneuver is displayed in Figure 9(a) with the spacecraft details in Table 6. The formation total maneuver ΔV is 13.18 m/s and the time of flight is 610 minutes. This long time of flight is reflected in the trajectories of the spacecraft in Figure 9(a); these trajectories "shadow" the paths of the targets for several revolutions before finally achieving the formation. This "shadowing" behavior is due to the influence of the J_2 perturbation on the spacecraft which is not modeled by the Yamanaka-Ankersen STM used in the MPC calculations; thus, a larger number of maneuvers are required to deliver all the spacecraft to their correct positions. Since the influence of Earth oblateness decreases with increasing distance from Earth, it is likely that the guidance algorithm will require less time of flight for a formation with a larger orbital radius.

Table 6. Maneuver Results for Figure 9(a)

	S/C 1	S/C 2	S/C 3	S/C 4
Target	C	A	D	B
ΔV [m/s]	3.14	3.41	3.15	3.43

The second simulation for this scenario uses the APF guidance scheme for delivery and, again, the ΔV weighting for the auction. The formation maneuver is presented in Figure 9(b) with the spacecraft particulars in Table 7. The guidance algorithm takes 362 minutes to achieve the formation with a total ΔV of 15.57 m/s. Once again, the APF guidance has a shorter time of flight but higher control cost when compared to the MPC example. The APF delivery method also uses the YA STM to plan maneuvers but is not as reliant as the MPC method on accurately predicting the future motion. This agnosticism to dynamics models is one of the advantages of APF guidance.

Table 7. Maneuver Results for Figure 9(b)

	S/C 1	S/C 2	S/C 3	S/C 4
Target	C	B	D	A
ΔV [m/s]	4.06	3.75	4.02	3.74

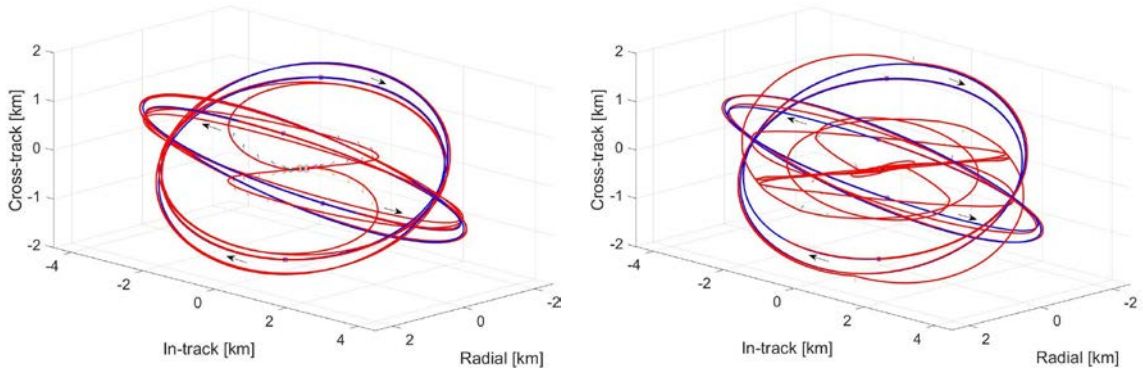

(a) MPC Formation Guidance **(b) APF Formation Guidance**

Figure 9. J_2 Deployment. Spacecraft Trajectories

The different colors shows the J_2 deployment spacecraft trajectories in Red, also the Target Trajectories is in Blue. Colored Arrows Indicate the Direction and Location of Impulsive Maneuvers, Black Arrows Indicate Direction of Motion

5 CONCLUSIONS

To summarize, the objective of this investigation is to create an autonomous, decentralized guidance algorithm for a formation reconfiguration maneuver of an arbitrary number of satellites. The algorithm must handle the twin problems of assignment and delivery. The current algorithm uses an auction process to assign the spacecraft to new positions in the formation. This auction bases its bidding around the estimated ΔV and the estimated time of flight for each transfer. The algorithm then uses either artificial potential functions (APF) or model predictive control (MPC) to design the maneuvers that deliver the spacecraft safely to its new position. The APF and MPC guidance strategies both utilize the Yamanaka-Ankersen approximation of orbital relative motion. In simulations under Keplerian and perturbed dynamics, the guidance algorithm is successful in guiding formations through reconfiguration maneuvers; it requires from the operator only the initial spacecraft state information and desired new formation geometry to perform the maneuver. Both APF and MPC have parameters that can be tuned to better suit different scenarios. Current work is focused on determining the optimal ranges of these parameters, along with which scenarios are suited to APF or MPC delivery methods.

6 RECOMMENDATIONS

Many challenges remain in the development of a fully decentralized autonomous guidance strategy for formation reconfiguration maneuvers. This investigation is preliminary and serves as the basis for more comprehensive developments incorporating specific spacecraft or mission limitations and requirements. Future efforts are likely to involve some combination for increasing the fidelity of the autonomous delivery methods, fully parallelizing the auction algorithm, and incorporating relative navigation concepts suitable for on-board implementation. Potential improvements in the autonomous delivery schemes include increasing the accuracy of the relative motion approximation used in the APF and MPC guidance schemes. The Yamanaka-Ankersen approximation is an improvement on the Clohessy-Wiltshire equations for elliptic reference orbits, however, it does not include any information on the non-spherical gravity perturbations. When the largest non-spherical term, J_2, is included in the dynamics, the performance of the MPC delivery scheme is impacted. There exist analytical approximations of relative motion under the J_2 perturbation (the Gim-Alfriend STM as one example) such that possible replacements for the YA STM in the APF and MPC schemes.[24] Alternative structures for the objective function used in the MPC delivery scheme also warrant more investigation. For example, the targeting of the modeled target final state $\mathbf{x}_k^*$ could be replaced by targeting the modeled target state at each of the $\mathcal{N}$ time steps.

The auction algorithm as currently designed slows the autonomous guidance algorithm, since it is currently run sequentially. A true "chief" spacecraft could be incorporated to run the formation and assign the deputy spacecraft to selected positions; however, to become more decentralized, it is desirable to spread the auction to various formation members and run it in parallel. The auction algorithm can be run in parallel and with delayed information sharing between the spacecraft.[25] The implementation would create a truly decentralized, autonomous guidance algorithm for the formation reconfiguration maneuver problem.

In an operation context, relative positioning errors leading to uncertainties between the spacecraft and obstacles, along with imprecise maneuver implementations, must be considered and addressed. The current investigation assumes perfect knowledge of the relative positions and velocities and does not accommodate maneuver errors. A process for incorporating relative state uncertainty would be beneficial as well as the sensitivities to these uncertainties. A Kalman filtering approach to uncertainty errors is a likely candidate for addressing the estimation problem. For errors in maneuver implementations, a minimum ΔV threshold on maneuvers would eliminate the large number of small thrusts recommended by both APF an MPC controllers. Alternatively, some investigation of a practical continuous controller is also warranted. A comprehensive examination of the most -suitable values for the various parameters in each delivery scheme is necessary for each specific mission application.

REFERENCES

[1] "About Prisma," http://www.lsespace.com/about-prisma.aspx. Accessed 2015-10-12.

[2] "ESA Science & Technology: Cluster," http://sci.esa.int/cluster. Accessed 2016-06-08.

[3] DeLee Smith, "The Magnetospheric Multiscale Mission," http://mms.gsfc.nasa.gov/about_mms.html. Accessed: 2015-10-12.

[4] "Terrestrial Planet Finder Interferometer," http://exep.jpl.nasa.gov/TPF-I/tpf-I_ index.cfm. Accessed 2015-10-12.

[5] "Darwin Overview," http://www.esa.int/Our_Activities/Space_Science/ Darwin_overview. Accessed 2015-10-12.

[6] M. Martin and M. Stallard, "Distributed Satellite Missions and Technologies—The TechSat 21 Program," *Space Technology Conference and Exposition*, Albuquerque, NM, 1999, pp. 28–30.

[7] D. P. Bertsekas, "The Auction Algorithm for Assignment and Other Network Flow Problems: A Tutorial," *Interfaces*, vol. **20**, no. 4, 1990, pp. 133–149.

[8] R. E. Burkard and E. Cela, "Linear Assignment Problems and Extensions," **Handbook of Combinatorial Optimization**, Springer, 1999, pp. 75–149.

[9] T. Wahl and K. C. Howell, "Autonomous Guidance Algorithm for Multiple Spacecraft and Formation Reconfiguration Maneuvers," *AAS/AIAA Spaceflight Mechanics Meeting*, Napa, CA, 2016, pp. 1939–1956.

[10] Wahl, T., "Autonomous Guidance Strategy for Spacecraft Formations and Reconfiguration Maneuvers," Ph.D. Dissertation, School of Aeronautics and Astronautics, Purdue University, West Lafayette, IN, December 2017.

[11] W. H. Clohessy and R. S. Wiltshire, "Terminal Guidance System for Satellite Rendezvous," *Journal of the Aerospace Sciences,* vol. **27**, September 1960, pp. 653–658.

[12] K. Yamanaka and F. Ankersen, "New State Transition Matrix for Relative Motion on an Arbitrary Elliptical Orbit," *Journal of Guidance, Control, and Dynamics*, vol. **25**, no. 1, 2002, pp. 60–66.

[13] O. Khatib, "Real-Time Obstacle Avoidance for Manipulators and Mobile Robots," *The International Journal of Robotics Research*, vol. **5**, no. 1, 1986, pp. 90–98.

[14] E. Rimon and D. E. Koditschek, "Exact Robot Navigation Using Artificial Potential Functions," *Robotics and Automation*, vol. **8**, no. 5, 1992, pp. 501–518.

[15] J. Muñoz, "Rapid Path-Planning Algorithms for Autonomous Proximity Operations of Satellites." Ph.D. Dissertation, University of Florida, Gainesville, FL, 2011.

[16] S. S. Ge and Y. J. Cui, "New Potential Functions for Mobile Robot Path Planning," *IEEE Transactions on Robotics and Automation*, vol. **16**, no. 5, 2000, pp. 615–620.

[17] S. S. Ge and Y. J. Cui, "Dynamic Motion Planning for Mobile Robots Using Potential Field Method," *Autonomous Robots*, vol. **13**, no. 3, 2002, pp. 207–222.

[18] M. Brand, V. Shilpiekandula, C. Yao, S. A. Bortoff, T. Nishiyama, S. Yoshikawa, and T. Iwasaki, "A Parallel Quadratic Programming Algorithm for Model Predictive Control," IFAC Proceedings Volumes, vol. **44**, no. 1, 2011, pp. 1031–1039.

[19] S. J. Wright, "Applying New Optimization Algorithms to Model Predictive Control," AIChE Symposium Series, vol. **93**, 1997, pp. 147–155.

[20] C. Jewison, R. S. Erwin, and A. Saenz-Otero, "Model Predictive Control with Ellipsoid Obstacle Constraints for Spacecraft Rendezvous," IFAC-PapersOnLine, vol. **48**, no. 9, 2015, pp. 257–262.

[21] D. P. Bertsekas and D. A. Castanon, "Parallel Synchronous and Asynchronous Implementations of the Auction Algorithm," *Parallel Computing*, vol. **17**, no. 6, 1991, pp. 707–732.

[22] M. M. Zavlanos, L. Spesivtsev, and G. J. Pappas, "A Distributed Auction Algorithm for the Assignment Problem," *Decision and Control,* 47th IEEE Conference, Cancun, Mexico, 2008, pp. 1212–1217.

[23] D. P. Bertsekas, **Linear network optimization: algorithms and codes**, MIT Press, Cambridge, MA, 1991.

[24] Dong-Woo Gim and Kyle T Alfriend, "State transition matrix of relative motion for the perturbed noncircular reference orbit," *Journal of Guidance, Control and Dynamics*, vol. **26**, no. 6, 2003, pp. 956-971.

[25] Michael M Zavlanos, Leonid Spesivtsev, and George J Pappas, "A Distributed Auction Algorithm for the Assignment Problem," *Decision and Control,* 47th IEEE Conference, Cancun, Mexico, 2008, pp. 1212-1217.

LIST OF SYMBOLS, ABBREVIATIONS, AND ACRONYMS

ΔV		Change in velocity magnitude, i.e., maneuver cost
J_2		Coefficient for the second zona harmonic, i.e., the 'oblateness' term, in the spherical harmonic representation of the Earth's gravitational field
$\hat{x}, \hat{y}, \hat{z}$		Cartesian coordinate direction in the Hill frame
$\boldsymbol{r}_c, \dot{\boldsymbol{r}}_c, \ddot{\boldsymbol{r}}_c$		Position vector from Earth center to chief vehicle and derivatives as viewed by an inertial observer
ECI		Earth Central Inertial coordinate frame
$\theta_c, \dot{\theta}_c$		True anomaly of chief in its orbit and tis rate of change
$\boldsymbol{\rho}, \dot{\boldsymbol{\rho}}, \ddot{\boldsymbol{\rho}}$		Position vector of deputy spacecraft relative to the chief and derivative as viewed by an inertial observer
x, y, z		Cartesian coordinates of position vector of the deputy relative to the chief
r_c		Magnitude of the position vector $\boldsymbol{r}_c$
$\boldsymbol{\omega}$		Angular velocity of the Hill frame with respect to the inertial frame
$\boldsymbol{r}_d$		Position vector from Earth center to the deputy vehicle
μ		Gravitational parameter for the Earth
E_c		Chief conic orbital energy
a_c		Chief orbit semi-major axis
E_d		Deputy conic orbital energy
p_c		Semilatus rectum of chief orbit
n_c		Mean motion of the chief orbit
$\mathcal{X}, \mathcal{Y}, \mathcal{Z}$		ECI coordinates for the
ϕ_a		Attractive potential
$\Phi(t_{k+1}, t_k)$		YA state transition matrix
$\mathcal{J}(\mathbf{U}_k, \mathbf{x}_k)$		Objective function for the MPC controller
$\mathbf{x}_k$		State of the spacecraft in the Hill fame
$\mathbf{U}_k = [\mathbf{u}_k, \mathsf{K}, \mathbf{u}_{k+\mathcal{N}-1}]^T$		Stacked vector of the controls $\mathbf{u}_k$, each at time t_k
$S, \mathcal{R}, \mathcal{V}, \mathcal{W}, \mathcal{K}$		Weighting matrices in guidance strategy
F, L		Weighting matrices n the auction algorithm
b_{ij}		Cost for spacecraft i to reach target j in the auction algorithm
p_j		Price of target j in the auction algorithm
$v_i, \quad \omega_i$		Minimum expense and second lowest expense in the auction algorithm
γ_i		Bid by spacecraft i in the auction algorithm

AAPF		Adaptive Artificial Potential Function
AFP		Artificial Potential Function
AFRL		Air Force Research Laboratory
CW		Clohessy-Wiltshire Model for Relative Motion
ECI		Earth Centered Inertial
DM		Delivery Method
ESA		European Space Agency
LVLH		Local-Vertical Local Horizontal
MMS		Magnetosphere Multiscale Mission
MPC		Model Predictive Control
NASA		National Aeronautics and Space Administration
NMC		National Motion Circumnavigation
PRISMA		Prototype Research Instruments and Space Mission Technology Advancement
STM		State Transition Matrix
TPF		Terrestrial Planet Finder
TOF		Time of Flight
YA		Yamanaka-Andersen approximation for the state transition matrix for relative motion

DISTRIBUTION LIST

DTIC/OCP
8725 John J. Kingman Rd, Suite
0944 Ft Belvoir, VA 22060-6218 1 cy

AFRL/RVIL
Kirtland AFB, NM 87117-5776 1 cy

Official Record Copy
AFRL/RVSV/Richard Erwin 1 cy